The Transient Performance of Partially-Undergrounded Overhead Lines in the Presence of Corona

Mohamed M. SAIED,
Life Senior Member, IEEE
Professor (Emeritus), Independent Researcher
Giza, Cairo EGYPT, m.saied@ieee.org

*Summary:*The paper presents a method for investigating the electromagnetic transients of partially under-grounded high voltage overhead transmission lines in the presence of corona. It is based on a time domain model in which the corona is simulated by distributed voltage-dependent shunt current sources. The line segments and the inserted cable section are represented by a single equivalent transmission element having location-dependent circuit parameters per unit length. The numerical solution of the resulting set of differential equations yields the distributions of the voltage, the longitudinal current and the shunt corona current (per unit length) as functions of location and time. The presented two-, three-dimensional and contour plots proved to be helpful in discussing these distributions and in identifying any eventual current and/or voltage concentrations. The developed computer code in *Mathematica* can handle any time waveform of the source initiating the transients, any line termination as well as any lengths of the overhead line and cable section.

I. INTRODUCTION

There is a noticeably growing interest in the concept of the partial undergrounding of high voltage networks comprising overhead transmission lines. It is defined as the replacement of parts of these lines by adequate sections of underground cables. This can lead to considerable economical and technical advantages, as detailed in [1-5]. Nevertheless, some important issues pertinent to these mixed power networks, such as the increased cost, the high cable charging capacitive reactive power, the cost of eventually required shunt reactors, as well as their impact on the power system's transient stability should be included in any meaningful feasibility study. Among the technical issues related to the partial undergrounding are the possible modifications in the steady state and transient voltage distributions, the increased secondary arc currents associated with the single-pole auto-reclosure and single-phase-to-ground faults as well as the impact on the networks' resonance frequencies which can coincide with those of some switching events [7].

The effect of the cable sections on the electromagnetic transients in high voltage networks has been investigated in several references such as [6-12]. They take into account the networks' topology, the lengths of the cable sections and the connections of the neutral points. Moreover, the ratio between the surge impedances of the different transmission elements has a significant effect on the voltage and current transients. Several studies, such as [7-12], deal with the analysis of the electromagnetic transients in typical partially-undergrounded power networks and assess the effectiveness of using cable sections in modifying the transients in the network components such as transformer substations. The analysis in [8] yields the transient voltage and current distributions along the partially undergrounded lines. Results can indicate any localized voltage and/or current concentrations. An exact direct analytical distributed

parameter approach to the modeling of the lines and cable sections is adopted. The non-uniform circuit parameters are represented by means of several step functions in terms of the coordinates. The resulting expressions are substituted in the simultaneous voltage and current differential equations, for which direct exact analytical solutions are available in terms of *Mathematica* parametric functions. The resulting Laplace s-domain voltage and current expressions will then be numerically inverted using the Hosono algorithm.

The study presented in [9] focuses on the effectiveness of using cable sections in reducing the transients in the power networks. A distributed parameter modeling of the overhead lines, underground cables and transformer windings is applied in the s-domain. The direct analytical s-domain solution is numerically inverted in order to get the corresponding time domain results. The affecting parameters such as the line and cable surge impedances, the length of the cable sections and the transformers' data, are investigated. A case study involving multiple-pulse lightning surges is also addressed.

Reference [10] addresses the integration of long 380kV cable sections, the transients resulting from their insertion and the effect of their large capacitances. The analysis of a sample 80km mixed line is conducted in the time-domain using PS CAD/EMTDC.

The studies [11, 12] deals primarily with the energization overvoltages in mixed networks with different circuit structures and their statistical distributions. It also addresses issues related to the insulation coordination.

The instantaneous voltage in certain regions of the overhead lines can exceed the corona onset value during some internal or external disturbances. This will accordingly modify the lines' equivalent circuits and their mathematical models in the way discussed in details in references [1] and [5]. They are based on simulating the distributed location–dependent corona discharge by suitable nonlinear shunt current sources.

To the best of the author's knowledge, no investigations have been conducted on analyzing the transients in partially-undergrounded lines with possible corona discharge.

This paper's main objective is, therefore, to present a method for the transient analysis of the mixed high-voltage overhead lines in the more general case of the simultaneous presence of both the partial undergrounding and the localized corona discharge.

The results of a parameter study will then be presented in order to demonstrate the effect of the line's termination and the circuit parameters of both the overhead lines and cable sections on the networks' transients. Moreover, the sensitivity of the electromagnetic transients to changes in the locations and lengths of the inserted cable sections will be discussed.

II. METHOD OF ANALYSIS
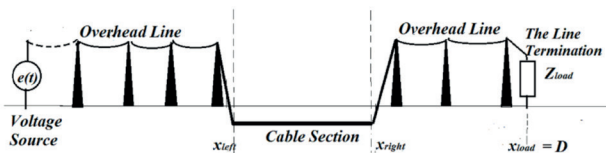
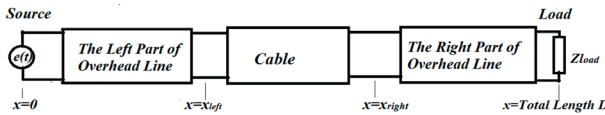Fig. 1. A sample mixed power network

Fig. 2. The equivalent circuit with three two-port networks

Consider the partially undergrounded overhead transmission line illustrated in Fig.1. It connects the voltage source $e(t)$, which initiates the line transients, with the terminals of the impedance load Z_{load}. The coordinates of the source and load terminals are denoted $x = 0$ and $x = x_{load} = D$, respectively. A part of the overhead line is replaced by a cable section inserted between the two junctions located at $x = x_{left}$, $x = x_{right}$. The classical approach to the analysis of this arrangement is to consider it as a cascade connection of three different two-port networks comprising the left part of the overhead line in the range $0 \leq x \leq x_{left}$, the cable section extending over $x_{left} \leq x \leq x_{right}$ and the right part of the overhead line with $x_{right} \leq x \leq D$. They are governed by three different sets of simultaneous differential equations. The circuit parameters per unit length of the two parts of the overhead line are the same. Kirchhoff's laws should be satisfied at the (line/cable) and (cable/line) junctions located at $x = x_{left}$ and $x = x_{right}$, respectively, as well as at the voltage source and load terminals. In the presence of corona discharge in some regions of the overhead line, distributed voltage dependent shunt current sources are added to the line model, as explained in references [1] and [5]. Due to the nonlinearity of corona phenomena, the time-domain analysis will be applied. The left and right parts of the overhead line are divided into a suitable number of sections or segments. Because of the relatively larger cable capacitance/unit length,
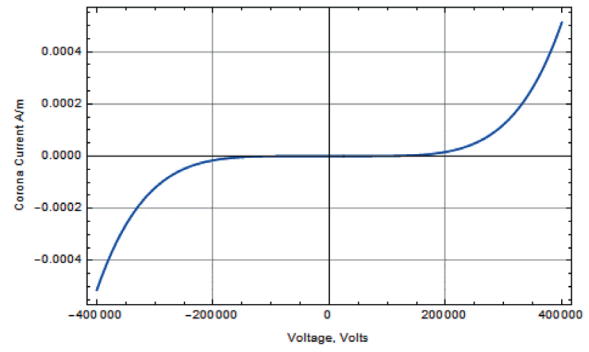

Fig. 3. The corona voltage-current characteristic for $k = 5$ and $a = 5 \times 10^{-32}$
X-axis: the voltage v, Volts
Y-axis: the corona current $i_{corona}(v) = 0.5 \times 10^{-31} \times v^5$, A/m

the cable is represented (in the classical approach) by a number of usually shorter segments.

The suitability of using the assumption

$$i_{corona} = a \cdot v_{corona}^k \qquad (1)$$

for describing the voltage-current characteristic of the corona discharge can be recognized from the corresponding plot in Figure 3 pertinent to the considered 400-kV line. In Eq. (1), i_{corona} and v_{corona} denote the corona current per meter, and the voltage at the considered overhead transmission line section, respectively. The value of k should be a positive integer number and greater than 1. The constant a depends on the atmospheric conditions, the line design and the conductors' surface conditions. The above equation can model a line section of a corona onset voltage of 160 kV.

The two constants a and k can be easily determined from the power frequency corona power loss measurements at two different voltages. Reference [5] uses the power loss in Watts per meter for a 3-phase line at the two rms line voltages 400 and 480kV. It indicates that the values $a = 5 \times 10^{-32}$ and $k = 5$ are suitable based on two corresponding 3-phase power loss measurements of 57 and 170W/m, respectively.

This paper suggests a more efficient approach for simulating such partially-undergrounded lines. The approach is based on replacing the three above-mentioned two-port networks shown in Fig. 2 by a single equivalent non-uniform line. The distribution of each of its circuit parameters can be expressed in terms of properly selected unit-step functions. These distributions can be written as follows:

$$r(x) = r_{line} + (r_{cable} - r_{line})[u(x - x_{left}) - u(x - x_{right})] \quad \text{(2-a)}$$

$$l(x) = l_{line} + (l_{cable} - l_{line})[u(x - x_{left}) - u(x - x_{right})] \quad \text{(2-b)}$$

$$c(x) = c_{line} + (c_{cable} - c_{line})[(u(x - x_{left}) - u(x - x_{right})] \quad \text{(2-c)}$$

$$a(x) = a_{line} + (a_{cable} - a_{line})[u(x - x_{left}) - u(x - x_{right})] \quad \text{(2-d)}$$

Where x_{left} and x_{right} are the coordinates of the left- and right-side line/cable junctions, respectively. The expressions $u(x - x_{left})$ and $u(x - x_{right})$ denote unit-step functions starting at $x = x_{left}$ and $x = x_{right}$. The terms r_{cable} and r_{line} are the
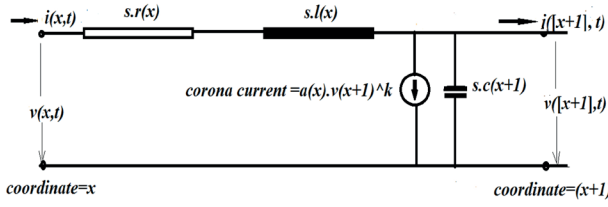
Fig. 4. The equivalent circuit of the segment of the transmission system between x and $(x + 1)$.

cable and line parameters/unit length, respectively. Similar definitions apply also for the inductance, capacitance and corona loss coefficient.

Based on the equivalent circuit depicted in Fig. 4, the two following differential equations for the voltage $v(x,t)$ and the current $i(x,t)$ can be obtained:

$$i([x + 1], t) = i(x, t) - s.c(x + 1).\frac{dv([x + 1], t)}{dt} - a(x + 1).v([x + 1], t)^k \quad (3)$$

$$v([x + 1], t) = v(x, t) - s.r(x).i(x, t) - s.l(x)\frac{di(x, t)}{dt} \quad (4)$$

from which expressions for the voltage and current time derivatives at any location x can be easily derived. The symbol $s = D/\text{Number of sections} = D/60$ in Fig. 4 and Equations (3), (4) denotes the length of one line segment (or section).

In the suggested approach, the coordinate x assumes only the integer values 0, 1, 2, .., D.

For instance, the four plots in Fig. 5 depict the functions $r(x)$, $l(x)$, $c(x)$ and $a(x)$ for a partially undergrounded 40-km 400-kV overhead line. Details of the line and cable data are given in the Appendix. In order to formulate the system of differential equations, the line is divided into 60 segments or sections, 666.67 m long each. This is the same for both the overhead line and the cable sections. In the particular case of Fig. 5, the cable replaces the overhead line between $x = x_{left} = 15$ and $x = x_{right} = 30$ sections.

The problem variables are 60 voltages (at points $x = 666.67$ m, 1333 m, 2000 m, etc. far from the sending end) and the series currents through the line or cable conductor at the same locations. A total of 120 differential equations are solved numerically using the software *Mathematica* (Version 11.3). The computer code utilizes the program NDSolve.

III. SAMPLE RESULTS

In general, results can be obtained for any line termination. The load should be simulated in the time-domain. Without any loss of generality, only the two extreme cases of open-circuit (or no-load) and short-circuit will be discussed. The source voltage is $e(t)$. The results are obtained for a step voltage of $e(t) = 400000\,u(t)$ volts. $u(t)$ is a unit-step function exhibiting a jump from the value zero to the value 1 at the time point $t = $ zero.
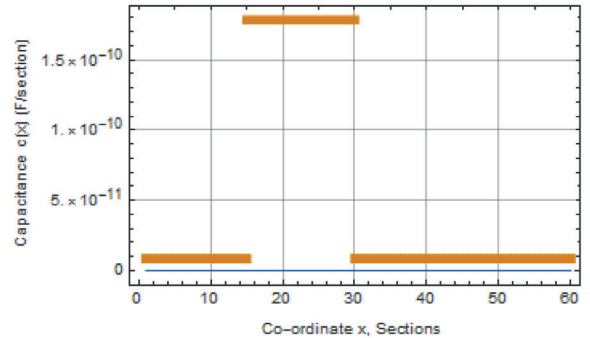
In the following case studies, it is assumed that a 13.333-km cable replaces the overhead line between the junctions at
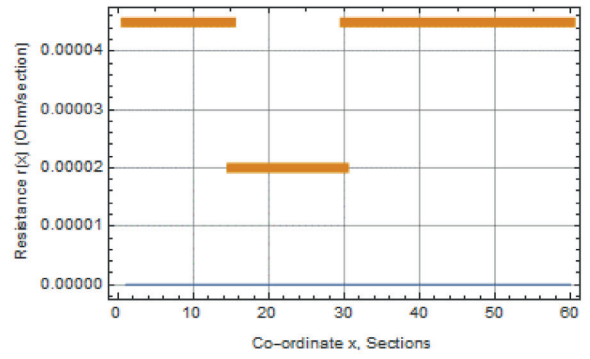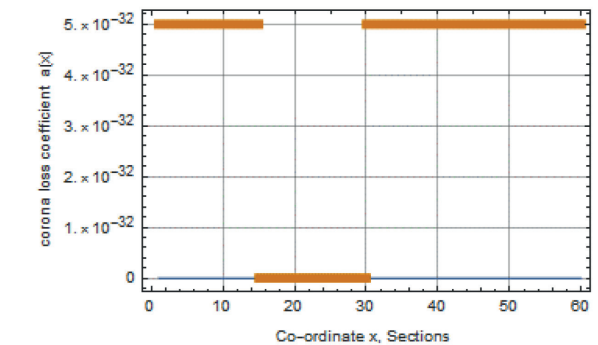

a) The resistance distribution $r(x)$
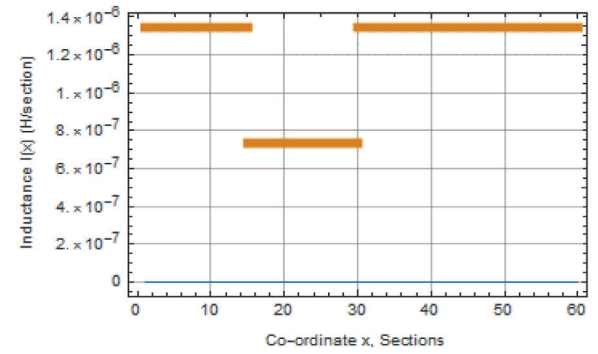
b) The inductance distribution $l(x)$

c) The capacitance distribution $c(x)$


d) The distribution of the corona loss coefficient $a(x)$

Fig. 5. The non-uniform distributions of the circuit parameters of a partially-undergrounded line over its entire length $0 \le x \le D$. The cable replaces the overhead line between $x = x_{left} = 15$ and $x = x_{right} = 30$ sections

3

$x = x_{left} = 15$ and $x = x_{right} = 35$. This corresponds to a cable length of 20 sections or segments.

Case Study (A): *Partially-Undergrounded Line With Corona at No-Load*

The plots in Fig. 6 illustrate the results of Case study (A). Figs. 6a and 6b show the receiving-end voltage and the (shunt) corona current/m close to the load terminal due to the 400-kV step voltage source, respectively. Plot 6a indicates that the receiving-end voltage starts to change from zero after a delay of about 240 µs which is longer than the intrinsic value $\tau = 133.33$ µs of the overhead line before undergrounding.

This is because of the slower propagation of the travelling wave along the cable. Due to the power dissipation of the corona and the conductor copper losses, the maximum value of the receiving-end voltage is only about 740 kV, which is 7.5% less than the theoretical value of 800 kV. The corona current time waveform in Fig. 6b indicates that it deviates from zero only after the receiving-end voltage exceeds the corona onset value of about 160 kV. It increases proportional to v^5, as assumed. Snapshots of the voltage and current waves along the line at the time point $t = \tau/2$, i.e. 66.667 µs, are depicted in Figs. 6c and 6d, respectively. It should be remembered that this time is sufficient enough for the voltage wave front to reach the left line/cable junction and to propagate
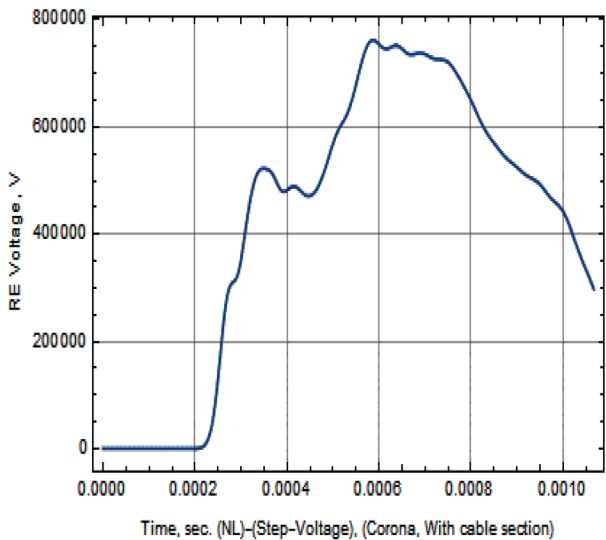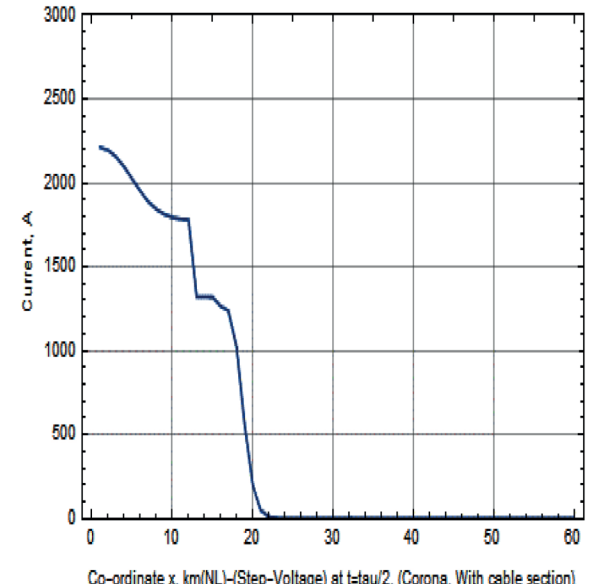

a) Voltage at receiving-end
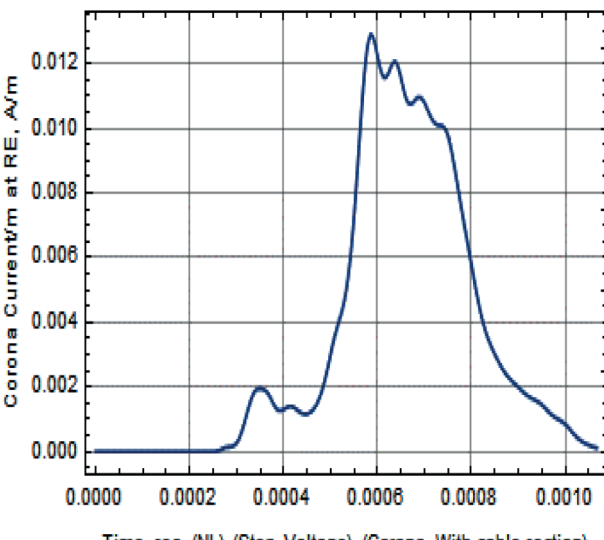
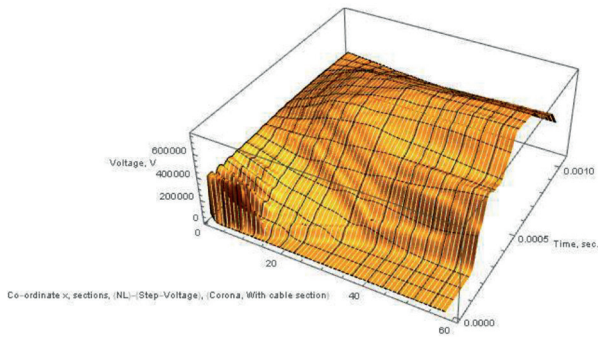b) Corona current/m close to the receiving-end
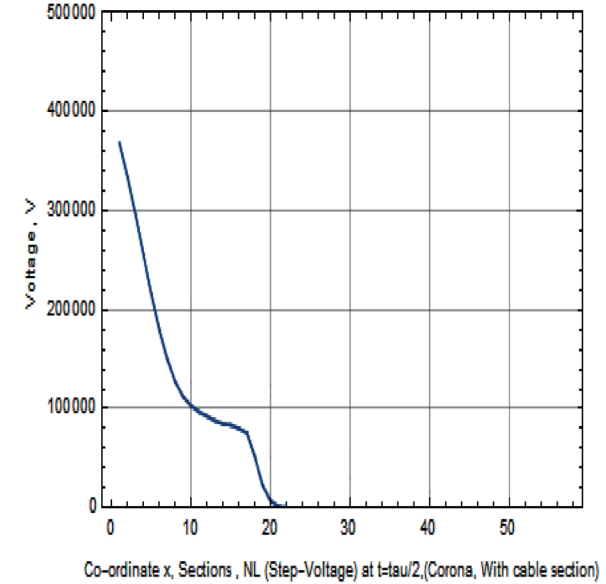
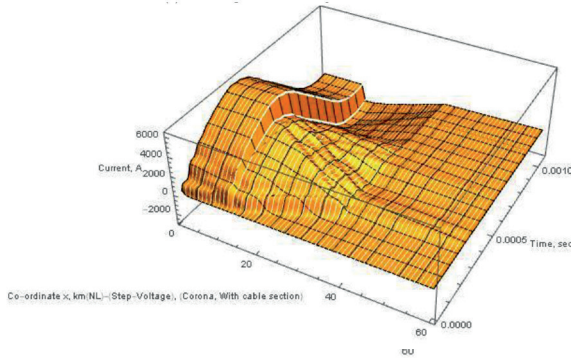c) Voltage distribution along the line at $t = \tau/2$

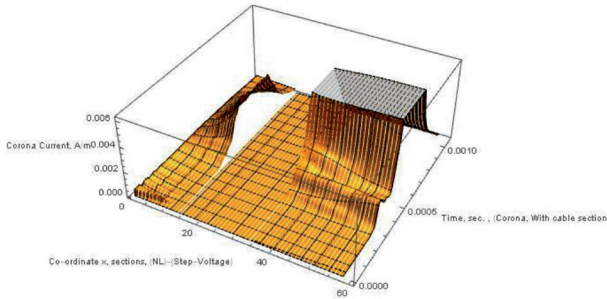

d) Current distribution at $t = \tau/2$

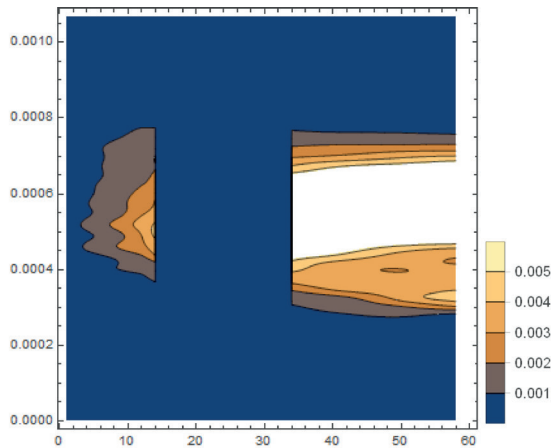Fig. 6. Results pertinent to Case Study (A)-Line Open-Circuited.

a) The 3-D plot of the voltage

b) The 3-D plot of the current

c) Tthe 3-D plot of the corona current.

d) The contour plot of the corona current.

The horizontal axis: The distance x from the source (measured in sections)
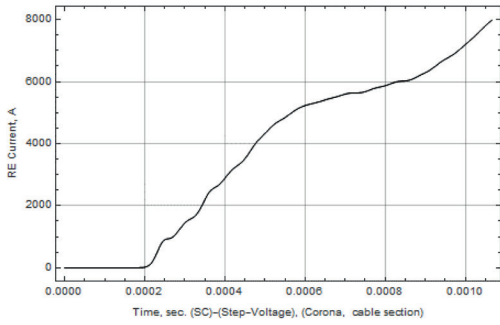The vertical axis: The corona current in A/section.

Fig. 7: Results pertinent to Case Study (A)-contd. -Line Open-Circuited

in the cable. The current range extends from approximately -2000 A to +6000 A. The deviation of the voltage and current wave fronts from the ideal step function is due to the copper losses (in the left part of the overhead line and in a part of the cable section), the corona losses (in the left part of the line) as well as the reflection at the left line/cable junction. It was noticed that relatively high voltage values prevail over most of the under-grounded line after about 600 μs. Furthermore the current exhibits high magnitudes at this time point especially near the source. The discontinuities due to the two line/cable junctions can be clearly recognized.

The three-dimensional plots a), b) and c) in Fig. 7 illustrate the voltage, current and corona current as functions of both the location (the x-axis) and the time (the y-axis) over the ranges $0 \leq x \leq 60$ segments and $0 \leq t \leq 1000$ μs. As expected, the sending-end voltage is always 400 kV, and the receiving-end current is always zero. The current remains very close to zero beyond the right cable/line junction, i.e. if $x \geq x_{right}$. It is noticed that the voltage will assume relatively high values over most of the under-grounded line after about 600 μs. This explains the large magnitudes of the corona current in this region, as manifested by the corresponding 3-D plot 7c) and the corresponding contour plot 7d), respectively. The corona current is exactly zero in the entire cable and in the regions of the overhead line where the voltage magnitudes are less than the corona onset value.

Case Study (B): Short-Circuited Partially-Undergrounded Line with Corona:

The plots in Fig. 8 depict the energization transient response of the previously described partially undergrounded line to the application of the 400 kV step voltage source. As the curve a) of the receiving-end current indicates, the total delay time of this composite line is approximately 240 μs. The current's average rate of rise is approximately 7.2 A/μs. This agrees with the value 400 kVolts/(0.040+0.013) Henries, where the 0.040 and 0.013 Henries are inductances of the overhead line (40 sections, 666.67 m each) and the cable (20 sections of the same length) connected in series. The 3-D plot of the voltage distribution in Fig. 8b) exhibits constant voltage values of 400 kV and zero at the supply terminals and the short-circuited receiving-end, respectively. After 1000 μs, the voltage decreases almost linearly from the source voltage to zero at the load. The 3-D current plot in Fig. 8c) exhibits always positive values. The current range is almost double that of the open-circuit case (A). The 3-D plot of the corona current (Fig. 8d) and the contour plot (Fig. 8e) indicate much smaller values in comparison with the corresponding plots (Figs. 7c and 7d) of the no-load case study (A). As shown by the legend of Plot 8e), the corona current/m ranges between zero and 0.00035 A/m. They are approximately 15 times less than those exhibited by plot 7d) of the open-circuit termination. This is because of the mostly smaller prevailing voltage magnitudes under short-circuit conditions. Similar to the open-circuit Case (A), the corona current is exactly zero in the cable and in the regions of the overhead line having voltages less than the corona onset value.
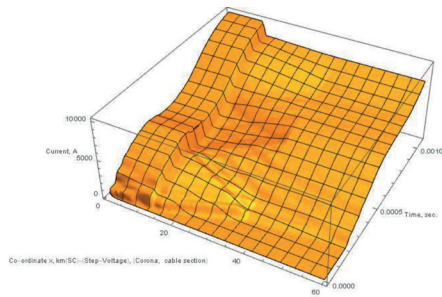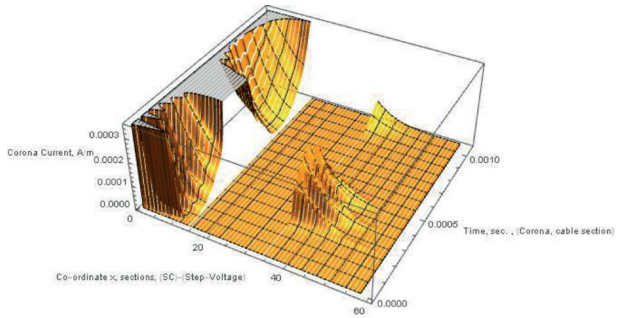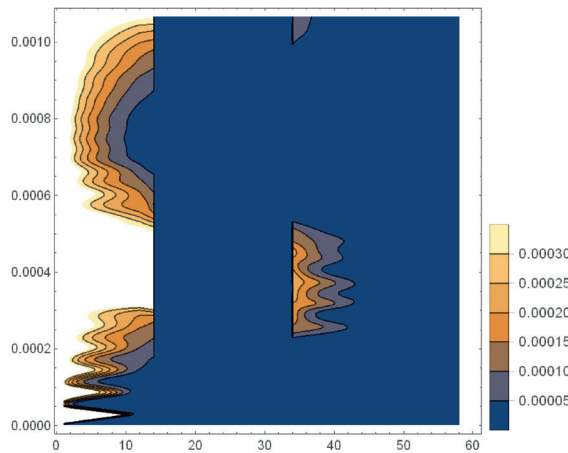
a) The receiving-end current
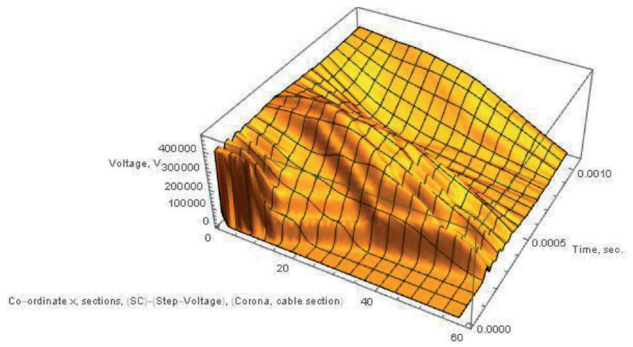
b) The 3-D voltage plot

c) The 3-D current plot

d) The 3-D corona current plot

e) The contour plot of the corona current
The horizontal axis: The distance x from the source (measured in sections)
The vertical axis: The corona current in A/section

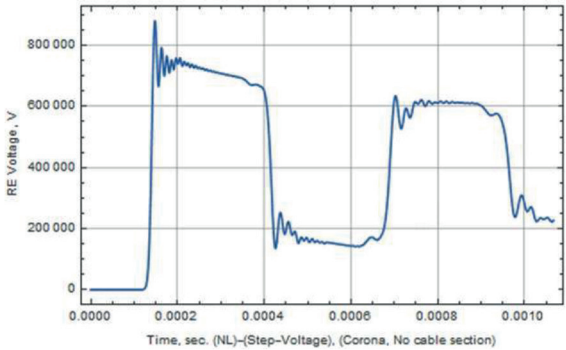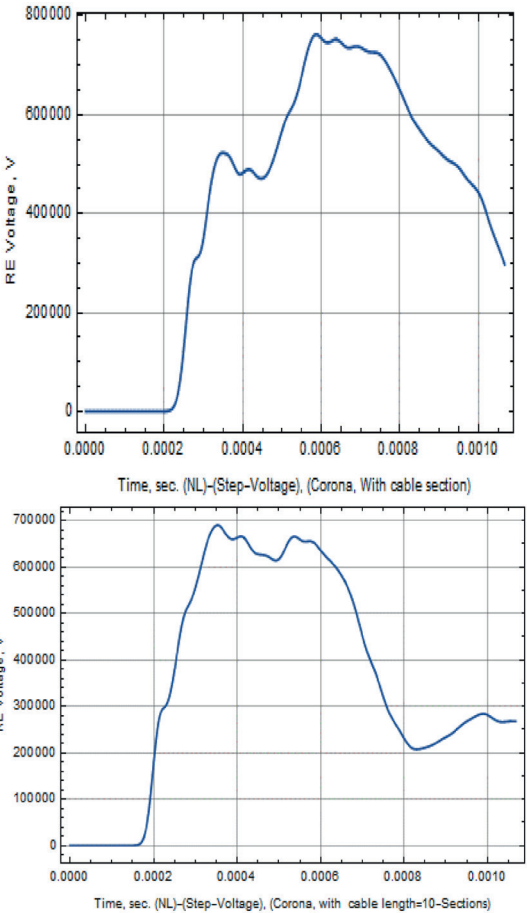Fig. 8. Results of Case Study (B) -Line Short-Circuited

Case Study (C): The Effect of the Cable Length

In this case study, it is assumed that a 6.6666-km cable is inserted between two junctions at $x = 15$ and $x = 25$. This corresponds to a cable length of 10 sections or segments. The line is open-circuited at its receiving-end. Samples of the results are presented in Fig. 9. The effect of the cable length can be discussed through the comparison of the sample plots of Fig. 9 with the corresponding ones shown in

Fig. 6 describing Case Study (A). Fig. 9a) illustrates the impact of reducing the cable length by 50% on the receiving-end voltage. With the shorter cable length (the plot on the right hand side), the voltage wave arrives at the load terminal after about 190 μs, i.e. about 10% earlier than Case (A) of the longer cable section. It can be also seen the peak transient voltage is approximately 690 kV, which is about 12% less than that of Case (A). The corona current with the shorter cable is shown in plot 9b). It should be compared with plot
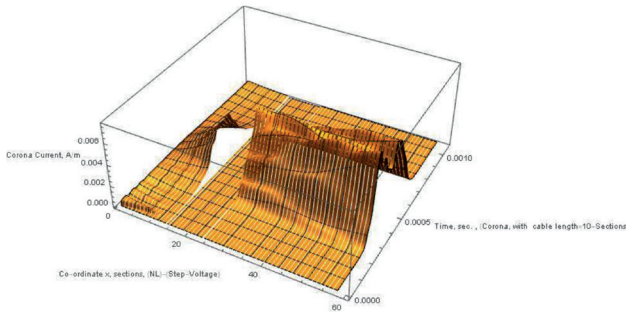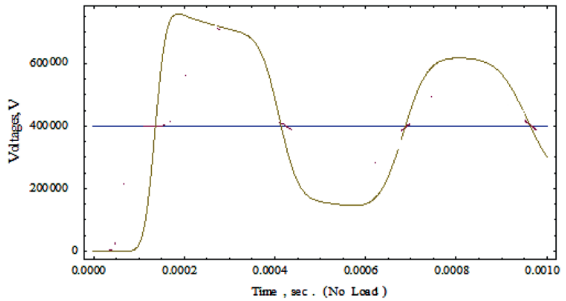
a) Voltages at receiving-end:
<u>Upper Plot</u> for a 13.333 km cable,
<u>Lower Plot</u> for a 6.666 km cable

b) The 3-D corona current plot

Fig. 9: Results pertinent to Case Study (C) -Line Open-Circuited with a 50% shorter cable, i.e. for a 6.666 km cable section

7c) pertinent to Case (A) dealing with the longer cable. They differ only between the right cable/line junction (i.e. $x = x_{right}$) and the line's receiving-end. In both cases, however, the maximum transient corona currents per unit length occur at a time point close to 600 μs, regardless of the location along the overhead line sections.

IV. MODEL VALIDATION

The three plots of Figure 10 will be used for validating the suggested technique. Plot a) illustrates the line's receiving-end voltage under corona but without any cable sections. The transients are initiated by a 400 kV step voltage and the line's end is assumed unloaded. Apart from the numerical Gibb's oscillations, this plot is in good agreement with the corresponding graph b) adopted from the Reference [5] for the same case study applying a completely different approach. Plot c) depicts the results for the case study involving no cable sections and no corona discharge. They agree with those obtained from investigating the wave propagation and reflections applying the Bewley lattice diagram [13].

a) Receiving-end voltage without cable sections, with corona considered

b) Receiving-end voltage without cable sections , with corona considered, adopted from Reference [5]
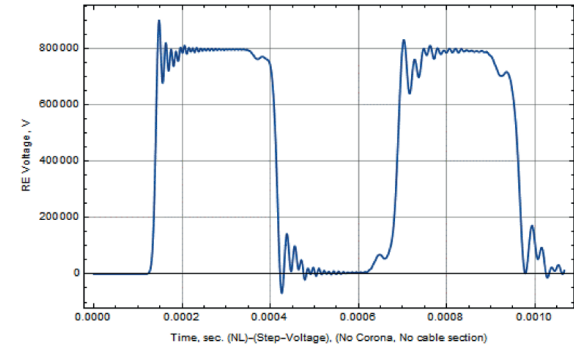
c) Receiving-end voltage without cable sections, without corona

Fig. 10. Model Validation

7

V. CONCLUSIONS

1. The concept of the partial-undergrounding of high-voltage overhead lines is discussed in view of the technical and economic considerations.
2. The need for investigating the transient performance of the partially-undergrounded lines in general and in the presence of corona discharge along parts of the overhead line in particular are pointed out and discussed.
3. The paper presents a method based on a time domain model in which the corona is simulated by distributed voltage-dependent shunt current sources.
4. The line segments and the inserted cable section are represented together by a single equivalent transmission element having location-dependent circuit parameters per unit length. This dependence could be efficiently expressed in terms of properly selected unit-step functions.
5. A program code is written in *Mathematica* 11.3 for solving the set of differential and algebraic equations. The solution gives the distributions of the transient voltages and currents as well as the shunt corona current per unit length along the mixed line.
6. The results of a parameter study are presented in order to demonstrate the effect of the line's load and the circuit parameters of both the overhead lines and cable sections on the networks' transients. The sensitivity of the electromagnetic transients to changes in the locations and lengths of the inserted cable sections is also discussed.

REFERENCES

1. Saied M., Safar Y., Salama M.: *Line Transients with Corona.* J. of the University of Kuwait (Science), vol. 14, no. 1, Jan. 1987.
2. Safar Y., Saied M.: *A model for simulating corona in the electromagnetic transients on transmission lines.* J. Computers and Electrical Engineering, vol. 29, issue 6, pp. 653-665, Aug. 2003.
3. Saied M., Safar Y.A.: *Electromagnetic transients on compensated lines under corona.* Electric Machines and Power Systems, vol. 16, no. 6, pp. 441-462, 1989, DOI:10.1080/07313568908909401
4. Naredo J., Soudack A., Marti J.: *Simulation of Transients on Transmission Lines with Corona via the Method of Characteristics.* IEE Proc Generat Transm Distrib, vol. 142, no.1, pp. 81-85, Jan. 1995.
5. Saied M.: *Corona Modeling for the Transient Analysis, Steady State and Corona Loss Performance of Transmission Lines.* Electrical Power Quality and Utilization J., vol. 16, no. 2, pp. 11-20, Dez. 2013.
6. Saied M.: *Effect of Cable Sections on the Electromagnetic Transients in Power Networks.* Electric Machines and Power Systems, vol. 15, no. 1, pp. 17-35, 1988.
7. Saied M.: *The Frequency Characteristics of Mixed Power Networks with Partial Undergrounding.* International J. of Power and Energy Research, vol. 1, no. 2, pp. 117-130, July 2017, DOI: 10.22606/ijper.2017.12004.
8. Saied M.: *The Electromagnetic Transients in Mixed Power Networks with Partial Undergrounding.* J. of Power Electronics and Power Systems, vol. 7, no. 2, pp. 1-13, 2017.
9. Saied M.: *Modifying the Transient Overvoltages in Mixed Power Networks by Inserting Cable Sections.* Electrical Power Quality and Utilization J., vol. 18, no. 1, pp. 7-14, Jun. 2015.
10. Khalilnezhad H., Popov M., L. van der Sluis, J. de Jong, N. Nenadovic N., Bos J.A.: *Assessment of Line Energization Transients when Increasing Cable Length in 380 kV Power Grids.* 2016 IEEE International Conference on Power Systems Technology, Sept. 28-Oct. 01, 2016, available online at https://www.researchgate.net/publication/309618106_Assessment_of_Line_Energization_Transients_when_Increasing_Cable_Length_in_380_kV_Power_Grids.
11. Khalilnezhad H., Popov M., Bos J.A., de Jong J.P.W., L. van der Sluis: *Investigation of Statistical Distribution of Energization Overvoltages in 380 kV Hybrid OHL-Cable Systems.* Proc. The Int. Conf. on Power Systems Transients (IPST2017), Seoul, Republic of Korea, available online at https://www.researchgate.net/publication/318225765_Investigation_of_Statistical_Distribution_of_Energization_Overvoltages_in_380_kV_Hybrid_OHL-Cable_Systems.
12. Khalilnezhad H., Popov M., L. van der Sluis, Bos J.A., Ametani A.: *Statistical Analysis of Energization Overvoltages in EHV Hybrid OHL-Cable Systems.* IEEE Trans. Power Del., vol. 33, no. 6, pp. 2765-2775, Dec. 2018.
13. Greenwood A.: *Electrical Transients in Power Systems,* 2nd ed., Wiley-Interscience, 1991, ch. 9.

APPENDIX

List of Symbols and Numerical Data
Line length = D = 40 km
Number of sections = 60
Overhead line's resistance/meter = r_{line} = 0.045 mΩ
Overhead line's inductance/meter = l_{line} = 1.346 μH
Overhead line's capacitance/meter = c_{line} = 8.55 pF
Overhead line's corona loss exponent = k = 5
Overhead line's corona loss coefficient = a = 5×10^{-32} Watt/m/V^k
Cable's resistance/meter = r_{cable} = 0.030 mΩ
Cable's inductance/meter = l_{cable} = 1 μH
Cable's capacitance/meter = c_{cable} = 0.1786 nF

Prof. Mohamed M. Saied
Received the B.Sc. degree (Honors) in Electrical Engineering from Cairo University, Egypt in 1965, then the Dipl.-Ing. and Dr-Ing. degrees from RWTH Aachen, Germany, in 1970 and 1974. From 1974 to 1983, he was at Assiut University, Egypt. In 1983, he joined Kuwait University where he served as full professor and EE Department Chairman. He spent one-year sabbatical leave (1998) as a Visiting Professor at Cairo University. Since his retirement in 2009, Prof. Saied works as an Independent Researcher, Giza, Cairo, Egypt. He is an IEEE Senior Member since 1984.